

1 **Pathological and Phylogenetic characterisation of *Amphibiothecum* sp. infection in an isolated**
2 **amphibian (*Lissotriton helveticus*) population on the island of Rum (Scotland)**

3

4 Caterina Fiegna¹, Charlotte L. Clarke^{*1,2}, Darren J. Shaw¹, Johanna L. Baily¹, Frances C. Clare²,
5 Alexandra Gray², Trenton W. J. Garner², and Anna L. Meredith¹

6

7 **Addresses**

8 ¹Royal (Dick) School of Veterinary Studies & The Roslin Institute, University of Edinburgh, Roslin,
9 EH25 9RG, UK

10 ²Institute of Zoology, Zoological Society of London, Regent's Park, NW1 4RY London, United
11 Kingdom

12 **Corresponding Author**

13 Charlotte L Clarke; E-mail: charlotte.wood@ioz.ac.uk

14 *Co-first Authors

15

16 Accepted for publication in *Parasitology*, published by Cambridge University Press. Available at:

17 <https://doi.org/10.1017/S0031182016001943>

18

19 **SUMMARY**

20 Outbreaks of cutaneous infectious disease in amphibians are increasingly being attributed to an
21 overlooked group of fungal-like pathogens, the Dermocystids. During the last 10 years on the Isle
22 of Rum, Scotland, palmate newts (*Lissotriton helveticus*) have been reportedly afflicted by unusual
23 skin lesions. Here we present pathological and molecular findings confirming that the pathogen
24 associated with these lesions is a novel organism of the order Dermocystida, and represents the first
25 formally reported, and potentially lethal, case of amphibian Dermocystid infection in the UK.
26 Whilst the gross pathology and the parasite cyst morphology were synonymous to those described
27 in a study from infected *L. helveticus* in France, we observed a more extreme clinical outcome on
28 Rum involving severe subcutaneous oedema. Phylogenetic topologies supported synonymy
29 between Dermocystid sequences from Rum and France and as well their distinction from
30 *Amphibiocystidium spp.* Phylogenetic analysis also suggested that the amphibian-infecting
31 Dermocystids are not monophyletic. We conclude that the *L. helveticus*-infecting pathogen
32 represents a single, novel species; *Amphibiothecum meredithae*.

33

34 **KEYWORDS**

35 Amphibiocystidium, Dermocystidium, Amphibiothecum, Palmate newts, Infection, Pathology,
36 Phylogenetics

37

38

39

40

41

42

43

44

45 **KEY FINDINGS**

- 46 • Here we characterise a novel amphibian pathogen infecting an isolated population of
47 palmate newts in Scotland.
- 48 • Using gross examination, histopathology, and molecular phylogenetics, we conclude that the
49 pathogenic agent belongs to a group of fungal-like organisms within the Dermocystida,
- 50 • Disease described on Rum represents a severe form of Dermocystid infection not previously
51 reported.
- 52 • We conclude that this novel organism, synonymous to the parasite described in palmate
53 newts in France, is a new species of amphibian infecting Dermocystid, part of the genus
54 *Amphibiothecum*.

55

56

57

58

59

60

61

62

63

64

65

66

67

68

69

70

71 INTRODUCTION

72 Amphibian populations have seen a dramatic global decline (Blaustein and Wake, 1990; 1995;
73 Houlihan *et al.*, 2000; Roelants *et al.*, 2007; Blaustein *et al.*, 2012), and amphibian infectious
74 diseases are key factors implicated in amphibian population declines (Berger *et al.*, 1998; 1999;
75 Lips, 1999; Daszak *et al.*, 2000). Most studies of amphibian infections focus on two pathogen
76 groups—chytridiomycete fungi (Densmore and Green, 2007; Lips *et al.*, 2006; Smith *et al.*, 2009)
77 and ranaviruses (Daszak *et al.*, 2000; Duffus and Cunningham, 2010). However, a rising number of
78 reports of amphibian infectious skin diseases have been attributed to a relatively poorly studied
79 group of organisms belonging to the order Dermocystidia (Class Mesomycetozoa: Pascolini, *et al.*,
80 2003; González-Hernández *et al.*, 2010; Rowley *et al.*, 2013; Raffel *et al.*, 2008). The order
81 Dermocystidia consists of pathogens known to infect mammals and birds (*Rhinosporidium* sp.)
82 (Herr *et al.*, 1999; Vilela and Mendoza *et al.*, 2012), fish (*Dermocystidium* spp. and Rosette agent)
83 (Ragan *et al.*, 1996; Mendoza *et al.*, 2002) and amphibians (*Amphibiocystidium* and
84 *Amphibiothecum* spp.) (Pascolini *et al.*, 2003; Feldman *et al.*, 2005). Due to their similar
85 morphology and explicit affinity to amphibian hosts, the amphibian-infecting Dermocystids were
86 considered a single genus (Pascolini *et al.*, 2003). However, the use of more advanced molecular
87 phylogenetics recently saw the reclassification of these pathogens into two distinct genera,
88 *Amphibiocystidium* and *Amphibiothecum* (Feldman *et al.*, 2005), which include some of the first
89 pathogens described in amphibians (Pérez, 1907; 1913), and are now known to be associated with
90 both caudate and anuran species (Pascolini *et al.*, 2003; Raffel *et al.*, 2008; Feldman *et al.*, 2005;
91 Densmore and Green, 2007).

92 In amphibians, Dermocystid infections manifest as spore-filled cysts (Pascolini *et al.*, 2003; Pereira
93 *et al.*, 2005; Raffel *et al.*, 2008; González-Hernández *et al.*, 2010) that macroscopically present as
94 small discrete cysts (~1mm) to larger multi-focal nodules. The limited data available suggests that
95 Dermocystid infection rarely causes mortality in amphibian hosts or population-level responses
96 (González-Hernández *et al.*, 2010; Densmore and Green, 2007). However, an association between

97 the presence of *Amphibiocystidium spp.* and declines in populations of *Notophthalmus viridescens*
98 (Raffel *et al.*, 2008) and *Pelophylax esculentus* (*Rana esculenta*; Pascolini *et al.*, 2003) has been
99 suggested.

100 In 2006, an unusual skin disease was reported in an isolated population of palmate newts (*L.*
101 *helveticus*) on the Isle of Rum, Scotland (Gray *et al.*, 2008), although anecdotal reports precede this
102 (Isle of Rum Rangers, *pers. comm.*, 2006). There are two described *Amphibiocystidium sp.* in
103 Europe; *A. ranae* known to infect green frogs (*P. lessonae* and *P. esculentus*) and a Dermocystid
104 infection affecting *L. helveticus* in France (Gonzalez-Hernandez *et al.*, 2010). Skin lesions affecting
105 newts on Rum bear strong resemblance to the latter. In both cases, newts of the same species
106 exhibited raised cystic to nodular cutaneous lesions. However, on Rum gross manifestations of
107 disease can appear more severe than those reported in France, and therefore, despite the similarity,
108 the pathogenesis and impact of this disease on the palmate newt population of Rum remains poorly
109 understood. Anecdotal reports from Rum suggest that, whilst some newts succumb to severe
110 infection, some populations are consistently free from infection (Anderson *et al.*, 2010). Anti-
111 microbial peptides (AMPs) produced by granular glands present in the skin of amphibians (Rollins-
112 Smith *et al.*, 2002; Zaslof, 2002) – part of the innate immune response – play an important role in
113 the first defence against microorganisms, and are increasingly being linked to the resistance of some
114 species to skin infecting diseases, such as Chytridiomycosis (Woodhams *et al.*, 2007; Rollins-
115 Smith, 2009). It is conceivable that gland function could extend to other fungal-like organisms and
116 gland structure should reflect any such interaction (Zaslof, 2002).

117 The classification of amphibian Dermocystids has largely been based on pathogen morphology
118 (Perez, 1907; Granata, 1919; Poisson, 1937; Jay and Pohley, 1981, Pascolini *et al.*, 2003). The
119 unusual fungal-like nature of these organisms, and differences in the terminology used in earlier
120 pathology descriptions, has led to uncertainty in their taxonomic placement. For example,
121 pathogens now considered to be from the same genus have previously been classified as both
122 protozoans (*Dermosporidium spp.*) and fungi (*Dermocycoides spp.*) (Perez, 1907; Granata, 1919;

123 Poisson, 1937; Jay and Pohley, 1981). DNA sequencing and molecular phylogenetics have been
124 important in resolving the taxonomic relationships of these similar, Dermocystid-like pathogens
125 described from amphibian hosts (Pereira *et al.*, 2005; Feldman *et al.*, 2005). Pereira *et al.*, (2005)
126 first used these techniques to analyse a small region of 18SrRNA from infected *P. esculenta* and *P.*
127 *lessonae*. Recovered topologies confirmed the pathogen to be a member of the Mesomycetozoeans,
128 and further supported the creation of a single genus, *Amphibiocystidium* (Pascolini *et al.*, 2003), to
129 incorporate amphibian-infecting pathogens previously classified as *Dermocystidium*, *Dermocoides*
130 and *Dermosporidium* (Pereira *et al.*, 2005). Feldman *et al.*, (2005) later reclassified this group into 2
131 genera, *Amphibiothecum* and *Amphibiocystidium*, based on the placement of *A. penneri* as a
132 member of the Mesomycetozoeans but distinct from other *Amphibiocystidium spp.* However, he
133 emphasised the limitations of the small gene region used for analysis and the small number of
134 known and sequenced Mesomycetozoeans, stating that increased sequence data for the
135 Dermocystids might improve the resolution and low bootstrap support (Feldman *et al.*, 2005).
136 Here the combined results of gross, histological and molecular investigations are presented,
137 characterising a novel dermocystid-like infection causing cutaneous disease in palmate newts on the
138 Isle of Rum, and providing phylogenetic support for the consideration of a new species within the
139 genus *Amphibiothecum*; *Amphibiothecum meredithae*. We conclude that disease on Rum represents
140 a severe case of Dermocystid-infection, and we examine the preliminary investigation into the
141 presence or absence of *Amphibiothecum sp.* and possible morphological differences in granular
142 glands (linked to AMP production and host innate immunity) that may play a role in the
143 susceptibility of skin infection.

144

145 **MATERIALS AND METHODS**

146 This study was carried out in May and June 2014 on the Isle of Rum (N57°00'55.1",
147 W006°16'53.3") Scotland, the largest of the Small Isles in the Inner Hebrides. The island is of

148 volcanic origin and contains numerous natural, dystrophic lakes and ponds that are the natural
149 habitat of the palmate newt (*L. helveticus*), the sole amphibian species present on the island.
150 One hundred and sixteen live adult newts were dip netted from three static water bodies. The
151 selection of sample sites was based on a previous study (Anderson *et al.*, 2010) and included one
152 pond (control site) where infection had not previously been recorded and no macroscopic cutaneous
153 lesions were observed during our sampling ($n = 12$ newts). The remaining 104 newts were captured
154 from the other two water bodies ($n = 51$ and $n = 53$). In addition, 23 dead newts were observed
155 around the banks of one infected site. Forty newts (28 from infected ponds and 12 from a control
156 site) were retained and transported live to the field station where they were euthanized. To do this,
157 newts were fully immersed in an aqueous solution of tricaine methane sulphonate (MS-222,
158 solution of 0.2% buffered with sodium bicarbonate) in accordance with the schedule 1 method
159 under the Animals (Scientific Procedures) Act 1986 and the American Veterinary Medical
160 Association guidelines and recommendations for ethical euthanasia of amphibians (AVMA, 2007).
161 Dermocystid lesions have previously been described on the skin of amphibian hosts, and on rare
162 occasions on the liver (Pascolini *et al.*, 2003; Raffel *et al.*, 2008; Feldman *et al.*, 2005; González-
163 Hernández *et al.*, 2010). A detailed external examination was performed where macroscopic dermal
164 lesions were recorded, detailing the size, colour and texture (Table 1), as well as noting their
165 abundance and distribution across the newt body. In order to retain the anatomical location of
166 visceral organs, a partial necropsy examination was performed and the coelomic cavity was
167 accessed via a ventral midline incision. The liver was fully exposed and, if present, cystic lesions
168 were recorded. Newts were then individually fixed by full body immersion in neutral buffered 10%
169 formalin. A further six newts with suspected Dermocystid-like lesions were humanely euthanised
170 by anaesthetic overdose as previously described and were immediately stored in 100% ethanol for
171 molecular analysis.

172 A subsample of 30 formalin-fixed newts, were processed for histological examination: 20 from
173 infected ponds (18 with lesions and 2 without) and 10 from the control site. Six axial sections of the

174 whole body were taken at predefined intervals; carcasses were sliced across the head (rostral to the
175 eyes and at the base of the skull), and across the trunk (at the level of the pectoral and pelvic girdles
176 and with two extra sections in between). The proximal third section of the tail, including the cloaca,
177 and fore- and hind-limbs were longitudinally oriented. Tissues were sectioned at 5 µm thick and
178 stained with hematoxylin and eosin (H&E) and examined by a light microscope for the presence of
179 parasitic cysts.

180 For transmission electron microscopy (TEM) analysis, one formalin-fixed skin tissue sample
181 containing multiple subcutaneous cystic lesions was deparaffinised, post-fixed in 1% osmium
182 tetroxide and processed routinely by dehydration through graded acetones prior to embedding in
183 araldite resin. Ultrathin sections (60 nm thick) were counterstained with uranyl acetate and lead
184 citrate and viewed with a Philips CM120 TEM. Images were taken on a Gatan Orius CCD camera.
185 To investigate the distribution and condition of cutaneous granular glands, across diseased ($n=16$)
186 and control newts ($n=8$), a standardised position was located in the tail dorsum (a segment just
187 caudal to the cloaca), that provided clear visibility of epidermal and dermal tissue in all newts and
188 adequate coverage of granular glands. These histological sections were photographed with a digital
189 camera (Olympus DP72) at 4 x magnification (approximately 2 mm long segment). The number
190 and diameter of all cutaneous granular glands in this section were assessed using Cell[^]D software
191 (Olympus Soft Imaging Solutions). Granular glands were considered mature when more than $\frac{3}{4}$ of
192 the gland alveolus was filled with bright eosinophilic granular material.

193

194 **Data analysis**

195 A logistic regression analysis was performed in R version 3.2.1 (R Core Team, 2015) to test the
196 hypothesis that cutaneous granular glands of the dorsal tail were different in those animals with
197 disease. The analysis was based on the infection status of the ponds (control, $n=8$; infected, $n=16$)
198 using a forward stepwise approach where the independent variables were: the number of cutaneous

199 granular glands, their diameters and the relative percentages of full glands, were entered into the
200 model with $p \leq 0.1$ and excluded with $p > 0.2$ (Hosmer and Lemeshow, 2000).

201

202 **Molecular Phylogenetics**

203 A sample of oedematous tissue (1mm²), a single dermal cyst or a single liver cyst was excised from
204 each of the 6 ethanol-preserved newts respectively. Excised tissue and cysts were washed in
205 deionized water and dried. DNA was extracted using DNeasy® Blood & Tissue Kit (Qiagen, UK)
206 according to the manufacturer's instructions.

207 Primers specific to the mesomycetozoean clade were designed, targeting a 1400bp region of 18s
208 rRNA, from an alignment of 5 Dermocystidia and Ichthyophonida 18s rRNA sequences sourced
209 from GenBank (*Dermocystidium* sp. CM-2002, AF533950; *Rhinosporidium seeberi*, AF118851;
210 *Ichthyophonus irregularis*, AF232303; *Ichthyophonus hoferi*, U25637, *Pseudoperkinsus tapestis*,
211 AF192386). Sequences were aligned using ClustalW (Larkin *et al.*, 2007). Conserved regions were
212 identified across the sequences to act as primers, ensuring enough variability in the target amplicon
213 to provide phylogenetic information. Both primers were compared to the online Basic Local
214 Alignment Search Tool (BLAST) (NCBI, online), confirming 100% homology with the
215 Mesomycetozoean species listed above and weaker homology with *L. helveticus* (84%, e-value
216 0.026). Polymerase chain reactions (PCRs) were performed in 25µl volume containing 1µg DNA,
217 0.3µM of each forward (5'-GTAGTCATATGCTTGTCTC-3') and reverse (5'-
218 TATTGCCTCAAACCTCCAT-3') primer, 200 µM dNTPs (Bioline, London, UK), and 2.5 units of
219 HotStarTaq Plus (Qiagen, Crawley, UK). Two µL of each PCR product were electrophoresed on
220 0.6% agarose gel, stained with GelRed™ Nucleic Acid Gel Stain (Biotium) alongside 2.5µL of a
221 1kb DNA Hyperladder™ (BioLine) to assess amplicon size. Amplification products of the correct
222 size were cleaned using Polyethylene glycol (PEG) precipitation, and commercially sequenced by
223 GATC Biotech. Sequences were manually edited in BioEdit (Hall, 1999) by trimming the outermost
224 5' and 3' ends near the sequencing primer site, where read quality was poor or ambiguous.

225 Edited sequences were aligned with all twenty-six 18S rRNA mesomycetozoean sequences
226 submitted in GenBank. Non-Mesomycetozoean out-group sequences were chosen based on high
227 query cover (98% ident.) but weaker similarity to the Rum isolate than the mesomycetozoean
228 sequences (<93%); JN054684.1, DQ9958071.1, KC488361.1. Sequences were aligned using
229 multiple sequence alignment in ClustalX2.1 (Thompson *et al.*, 1997).

230 Maximum likelihood analysis and Bayesian analysis have different strengths and may return
231 different topologies due to random errors in tree reconstruction (Svennblom *et al.*, 2006; Yang and
232 Rannala, 2012). For that reason, phylogenetic relationships were generated using both Maximum
233 Likelihood and Bayesian analysis to compare the topologies recovered and therefore offer more
234 support to the relationships and clades recovered by both analyses. MrModelTest (Posada and
235 Crandall, 1998) was performed in PAUP* 4.0 (Swofford, 2002), testing 56 different models of
236 DNA evolution against a starting Neighbour-joining tree. The best-fit nucleotide model as
237 determined by the Bayesian information criterion (BIC) (Schwarz, 1978; Ripplinger and Sullivan,
238 2007) was Hasegawa-Kishino-Yano (Hasegawa *et al.*, 1985) with gamma distributed rate variation
239 and invariable sites (HKY+G+I). Maximum likelihood analysis was performed in Paup*4.0
240 (Swofford, 2001) setting parameter values as detailed above, and specifying the outgroup. Analysis
241 was run with 1000 bootstrap iterations of a heuristic search and tree-bisection-reconnection (TBR)
242 branch swapping (Posada and Crandall, 1998). So as not to restrict model selection to named (*i.e.*
243 Jukes and Cantor) or pre-specified models, model averaging was implemented for Bayesian
244 analysis, sampling among the 203 general time reversible (GTR) models (Huelsenbeck *et al.*, 2004).
245 This was achieved by running analysis using the reversible-jump Markov chain Monte Carlo (rj-
246 mcmc) in MrBayes 3.1.2 (Ronquist and Huelsenbeck, 2003), specifying gamma distributed rate
247 variation, running 2 independent metropolis-coupled MCMC with 4 chains each, terminating after
248 10,000 replications when the standard deviation between the split frequencies reached <0.01
249 (indicating that the trees being sampled have converged), sampling every 100. Final consensus trees

250 were edited in FigTree v1.4.2 (Rambaut, 2014) adding bootstrap values or bipartition posterior
251 probabilities.

252

253 **RESULTS**

254 **Gross Pathology**

255 A total of 66 newts with macroscopic cutaneous lesions, suggestive of Dermocystid-like infection
256 as described by González-Hernández et al., (2010), were recovered from two ponds; prevalence of
257 47% (95%CI [34, 60]) and 76% (95%CI [64, 87]) respectively. Of the 23 dead newts found, six
258 were sufficiently well preserved to see that they had extensive dermal lesions, similar to those seen
259 in live newts described hereafter.

260 Ninety-three per cent (26/28) of newts (15 male and 13 female) subject to detailed external
261 examination had macroscopic lesions of all types (*e.g.* A, B, C and D; Table 1). The shape of skin
262 lesions varied depending on the number and size of parasitic cysts and the associated subcutaneous
263 oedema, whereas the shape of parasitic cysts were consistently spherical and pale grey/white.

264 Additionally, subcutaneous haemorrhage and circular skin ulcers (up to 6 mm in diameter) were
265 observed affecting fourteen (54%) newts; these were clustered over the tail, limb insertions and
266 subgular regions. Parasite cysts and skin lesions were most frequently observed on the dorsal

267 surface of the body ($n = 23$). More specifically, cysts were located on the heads ($n = 16$), tails ($n =$

268 20), limbs ($n = 20$) and subgular regions ($n = 18$) along with solitary or multiple type A lesions on

269 the liver ($n = 11$). Four newts (2 female and 2 male) (15%) had additional, severe and diffuse

270 subcutaneous oedema associated with cutaneous depigmentation and presence of numerous type D

271 lesions. These animals were moribund or showed limited body movements prior to euthanasia.

272

273 **Histology and TEM**

274 Histopathological examination confirmed the presence of parasite cysts, or related pathological
275 changes in newts ($n=20$) from infected ponds including the two individuals that had no
276 macroscopic skin lesions.

277 Single or multiple, intact or ruptured spheroid parasite cysts were consistently present expanding
278 the *strata spongiosum* and *compactum* of the dermis (Fig. 1). Cysts were also present in the
279 subjacent skeletal muscular layers (epi- and perimysium; $n=10$ newts), oral mucosa ($n=5$ newts),
280 gastrointestinal lumen ($n=1$ newt), liver ($n=7$ newts) and cloaca stroma ($n=3$ newts). See
281 Supplementary figure 1A-D.

282 Based on cyst morphology and the associated host's inflammatory response (Fig. 2A-D) we could
283 identify 3 different developmental stages: 1) developing (intact), 2) mature (intact and ruptured) and
284 3) degenerating and degenerated parasite cysts. All stages were observed concurrently affecting the
285 same individual. Developing cysts were associated with no, or a mild, host cellular response (Fig.
286 2A) whereas ruptured and mature cysts were associated with tissue oedema and moderate to severe
287 focal chronic-active inflammatory cell infiltrate. In addition, multinucleated giant cells (foreign
288 body-type cells) and focal tissue necrosis (Fig. 2B) were occasionally present. In cases of severe
289 subcutaneous swelling, numerous and generally ruptured parasitic cysts were present (up to 55),
290 surrounded by a moderate chronic-active inflammatory cell infiltrate and tissue oedema.

291 Degenerating cysts (Fig. 2C) were comparatively smaller and were characterised by a corrugated
292 and convoluted cyst wall, partially or fully detached from the host connective tissue. A focal
293 chronic-active inflammatory host response surrounded degenerating cysts and their lumen
294 contained an amphophilic to brightly eosinophilic granular matrix admixed with irregular islands of
295 pale basophilic material reminiscent of endospore formations. The advanced stage of cyst
296 degeneration (degenerated cyst) (Fig. 2D) was characterised by a focal granulomatous lesion
297 formed by packed mononuclear cells admixed with multinucleated giant cells, centred on a remnant
298 of collapsed cyst wall. The majority of the parasitic cysts observed in the liver (84%) were either

299 ruptured or degenerated, and were surrounded by a dense chronic inflammatory cell infiltrate
300 admixed with several multinucleated giant cells (foreign body-type cells)(Fig. 2E-F).
301
302 Intradermal developing cysts appeared as spherical sporangia ranging in size from 250 μm to 1.7
303 mm in diameter separated from the host connective tissue by 2-6 μm thick eosinophilic cyst walls
304 (Fig. 3A). These contained a myriad of basophilic developing immature endospores (IE). IE were
305 polygonal to crescent shaped, measured approx. 6 μm in diameter and had amphophilic to
306 basophilic, occasional vacuolated, protoplasm depending on the stage of development. IE were
307 packed within round to oval and refractile (“mucoid-like”) chambers ranging in size from 10 to 40
308 μm in diameter (average approx. 24 μm), formed by clusters of dividing and budding elements
309 further separated by internal faintly distinguishable septa (Fig.3 B). Depending on the stage of cyst
310 maturation, IE were present along with a variable number of mature endospores (ME); clusters of
311 IE or ME were observed either at the centre or at the inner periphery of the cyst wall within the
312 same cyst (Fig. 3C). ME were located within less well-demarcated and comparatively smaller
313 internal chambers, were round to ovoid measuring on average approx. 15 μm in diameter and were
314 stained deeply basophilic. In the later stage of cyst maturation, ME (hereafter granular mature
315 spore) were characterised by eosinophilic protoplasm swamped by numerous sub-spherical (approx.
316 1 μm in diameter) basophilic granular bodies. Granular mature spores were found within the lumen
317 of mature cysts or were noted as free forms or engulfed by macrophages in the contiguous host
318 tissues (Fig 3 C and D). When observed at higher magnification, granular mature spore resembled
319 clusters of merozoite elements budding from the surface of mature shizonts (Fig 3 D). No flagellae
320 or other motility organelles were observed.

321 Ultrastructural (TEM) examination of an intradermal cyst revealed endospores as an individual unit
322 enclosed in a thick electron dense fibrous and granular matrix delimiting outer endospore capsule
323 (Fig. 4). The endospore protoplasm was further enclosed by an additional, non-uniformly
324 distributed granular coat formed by convoluted membranes. The protoplasm of larger endospores

325 was further subdivided through a process of invagination of these internal delimiting membranes,
326 where the outer matrix eventually enclosed them into distinct subunits. Dividing endospores
327 contained between 2 to 4 daughter cells (Fig. 4A, insert).

328

329 **Tail granular Glands**

330 The number of cutaneous granular glands of the dorsal tail skin in the control group ($n=8$) ranged
331 from 7 to 14 (mean 10.4 ± 2.5). On average, 79% of tail glands were mature. Gland diameters
332 ranged from $53.3 \mu\text{m}$ to $401.0 \mu\text{m}$ (average $204 \pm 80 \mu\text{m}$). The number of glands in infected newts
333 ($n=16$) ranged from 8 to 28 (mean 13.4 ± 4.3) with their diameter ranging from 27.1 to $489.8 \mu\text{m}$
334 (mean 147 ± 90). On average 50% of glands in the tail skin of infected animals were classified as
335 mature. Step-wise regression analysis indicated that infected newts had marginally smaller glands
336 than non-infected newts ($\beta = -0.025$, 95% CI $[-0.047, -0.023]$, $p < 0.031$).

337

338 **Molecular analysis**

339 Successful amplification of a 1400bp DNA fragment was achieved from all DNA extractions.
340 Retrieved sequences from samples representative of liver and dermal cysts and subcutaneous
341 oedema were identical, confirming that each of these distinct pathologies are associated with the
342 presence of the same pathogen. These sequences shared high nucleotide similarity ($>94\%$
343 similarity, $>81\%$ query cover) to members of the Mesomycetozoeans. Upon alignment with all
344 Mesomycetozoean 18srRNA sequences archived in Genbank, nearly complete consensus was
345 observed (1bp difference) between Rum and two Dermocystid sequences isolated from infected *L.*
346 *helveticus* in France (Dermocystid-Larzac; accession numbers GU232542.1 and GU232543.1).
347 Overall the topologies obtained by Bayesian and Maximum Likelihood techniques were congruent,
348 although some differences in the internal relationships between *Dermocystidium sp.* and
349 *Amphibiocystidium sp.* were recovered. Both Bayesian and Maximum Likelihood analysis
350 confirmed the Rum parasite to be a member of the Dermocystids, forming a well-supported clade
351 with sequences from infected *L. helveticus* sampled in Larzac (Fig 5: BS = 99.4%; PP = 0.7.)

352 Whilst the *Rhinosporidium sp.* formed a monophyletic clade, the amphibian-infecting
353 Mesomycetozoeans were polyphyletic. Under both analyses a clade was recovered suggesting a
354 sister relationship between *A. penneri* and sequences from Rum and Larzac. Despite relatively weak
355 confidence in this relationship (PP = 0.7; BS = 58.2%), support for a split between this clade and
356 the rest of the Mesomycetozoeans was extremely high (BS = 100%; PP = 1.0.).

357 **DISCUSSION**

358 This study reports combined gross, histopathological, ultrastructural (TEM) and molecular findings
359 that characterise *Amphibiothecum sp.* infection in a geographically isolated population of palmate
360 newts on the Isle of Rum (Scotland). Whilst we can say little about the prevalence of infection
361 across the island from our sample of three water bodies, 63.5% of sampled live newts from infected
362 ponds showed signs of disease, indicating that infection is likely to be common in palmate newts on
363 the island.

364 As observed microscopically and ultrastructurally, intradermal parasitic cysts shared many common
365 features with other Dermocystic organisms (Broz and Privora, 1952; Jay and Pohley, 1981;
366 Gonzalez-Hernández *et al.*, 2010), in particular with that described in palmate newts in France
367 (Gonzalez-Hernández *et al.*, 2010). Similar to their observation, we also noted the presence of
368 numerous endospores organised in internal, septated chambers enclosed by a cyst wall. Within the
369 same cyst, clusters of endospores were observed at different developmental stages where the
370 smallest compartmented chambers enclosed 2-4 single endospore elements. However, the
371 arrangement of IE within mature cysts differed from that described by Gonzalez-Hernández *et al.*,
372 (2010) where the authors propose a centrifugal fashion of endospores maturation. Instead, in this
373 study, IE were present in clusters closer to the inner cyst wall of developed cysts and not
374 exclusively at the centre of the cyst (Fig. 2C). This finding therefore suggests a different pattern of
375 endospore maturation and a potential mechanism of endospores release. One possibility is that fully
376 matured endospores escape in a “programmed” pattern as described for *Rhinosporidium seeberi*

377 (Mendoza *et al.*, 1999), where endospores might develop toward the cyst's pore from where they
378 are discharged. However, we were unable to identify a cyst pore in any of the histological sections.
379 In agreement with other amphibian-specific Dermocystid infections (Pascolini *et al.*, 2003; Pereira
380 *et al.*, 2005; Raffel *et al.*, 2008; Hernandez-Gonzales *et al.*, 2010 and Courtois *et al.*, 2013).
381 diseased newts on Rum had macroscopic distinctive, raised, pale-white cystic skin lesions. In
382 contrast to what was observed from *Dermocystidim* spp. infection of *Rana temporaria* and *P.*
383 *esculenta* (Guyénot and Naville, 1922; Pascolini *et al.*, 2003) and *Amphibiocystidium* sp. infection
384 in Eastern red-spotted newt (Raffel *et al.*, 2008), here no "U" or bent "C" shaped cysts were seen.
385 In addition, we frequently observed unusually large subcutaneous fluid filled vesicles/bulla (e.g.
386 type D lesion) accompanied with full body oedema as a result of *Amphibiothecum* sp. infection.
387 Similarly to *Amphibiocystidium* sp. infected newts in France (Gonzalez-Hernández *et al.*, 2010), we
388 observed skin lesions primarily distributed over the newt dorsum, limbs and tail, and only
389 occasionally over the ventral trunk. This is in contrast to other *Amphibiocystidium* spp. infections
390 where cyst distribution was often concentrated on the ventral surface (Broz and Privora, 1951;
391 Densmore and Green, 2007; Pascolini *et al.*, 2003; Pereira *et al.*, 2005; Raffel *et al.*, 2008).
392 The presence of parasitic cysts at different developmental stages, and the related pathological
393 changes (as observed grossly and histologically), are together suggestive of infection progression.
394 While intact developing cysts were characterised by absent or a mild host inflammatory response,
395 fully mature and ruptured cysts were always associated with a discrete inflammatory response. In
396 the latter stages of cyst degeneration, granuloma formation resulted in reduced tissue inflammation
397 and the restoration of surrounding tissues. Similarly, following the hepatic dissemination,
398 granulomatous lesions commonly occurred. Although not the primary focus of this study, we
399 suggest that the cyst wall plays a crucial role in protecting the parasite from the host immune
400 system during its development. In fact the virtual absence of an inflammatory response surrounding
401 intact developing cysts is noteworthy in comparison to the inflammation surrounding ruptured and
402 degenerating cysts. Clinical manifestation of *Amphibiothecum* spp. infection in palmate newts on

403 Rum varied from subclinical (*e.g.* apparently healthy individuals with only few microscopic
404 subcutaneous parasitic cysts), up to severe generalised infection. While the processes causing
405 different clinical outcomes remain unclear, these observations suggest that whilst some newts may
406 recover from *Dermocystid* infection (*e.g.* presence of microscopic dermal resolving lesions), other
407 individuals develop a generalised and potentially fatal disease.

408 Here we described animals with microscopic parasite cysts, without the presence of gross lesions.
409 Gonzalez-Hernandez *et al* (2010) found no evidence of asymptomatic or carrier-state individuals
410 from infected palmate newts in France, however, the presence of *A. viridescens* cysts were observed
411 on the livers of apparently uninfected Easter red-spotted newts (Raffel *et al.*, 2008). This suggests
412 that subclinical infection might be more common than expected and the observation of macroscopic
413 skin lesions alone may not be a good proxy to determine infection prevalence. The detection of
414 pathogen genomic DNA from toe or tail clippings, and skin, oral or cloacal swabs, offer alternative
415 detection methods extensively employed for Bd and Ranavirus surveillance (Annis *et al.*, 2004;
416 Hyatt *et al.*, 2007; Skerratt *et al.*, 2008; Goodman *et al.*, 2013). However, the validity and accuracy
417 of these methods are being questioned. Whilst swabbing techniques have been found to
418 underestimate both infection prevalence and parasite burden in Chytridiomycosis (Shin *et al.*, 2014;
419 Clare *et al.*, 2016), they will often miss subclinical Ranvirus infections (Greer and Collins, 2007;
420 Gray *et al.*, 2012). Detailed histopathological examination therefore represents an important
421 diagnostic tool, particularly in cases of seemingly healthy individuals with only subclinical disease.
422

423 Severe full body oedema was microscopically associated with a high parasite burden along with a
424 generalised form of infection evidenced by concurrent presence of cysts in the liver. To the authors'
425 knowledge, this is the first published report of a generalised *Dermocystid spp.* infection, which
426 results in severe subcutaneous oedema as confirmed by both histopathological and molecular
427 analysis. Subcutaneous oedema would likely result from osmotic and electrolytic imbalances

428 caused by extensive breaches in skin integrity due to numerous presence of parasite
429 cysts in the liver might also result in hepatic insufficiency and systemic disease.
430

431 In addition to skin (mainly present within the dermis) and hepatic lesions, parasite cysts were also
432 found in previously unreported body sites such as oral mucosa, intestinal lumen, cloaca and
433 infiltrating within the skeletal muscle bundles. Secondary skin lesions were also occasionally
434 observed from infected newts and consisted of skin ulcers and haemorrhages as previously reported
435 (Gonzalez-Hernandez *et al.*, 2010). We consider that secondary lesions resulted from self-induced
436 trauma, and from weakening or breaches of the epidermis associated with parasite cysts.

437 Altogether these findings suggest that the intensity of infection may be critical in determining the
438 outcome of disease. Severe infection could increase mortality either directly, or indirectly by
439 compromising newt fitness (*e.g.* reducing foraging and motility capabilities) or by rendering
440 diseased newts more vulnerable to predation by compromising locomotion (Lindstrom, *et al.*,
441 2003). The presence of lesions in the oral mucosa could impact food intake, whereas cysts and
442 oedema on the cloaca could have an impact on breeding and courtship. If cysts and oedema on the
443 cloaca are a common finding the ability of male to produce spermatophores may be compromised.
444 Similarly breeding success may also be reduced in other ways; male newts rely on tail fanning to
445 entice females and lead them over deposited spermatophors (Halliday, 1990; Griffiths, 1996),
446 behaviours that may be hindered considerably by the presence of tail oedema or significant lesions.
447 Since the majority of *Amphibiothecum spp.* cysts were found within the dermis or adjacent tissues
448 (*e.g.* skeletal muscles bundles), parasite transmission is likely to occur by direct skin exposure to
449 contaminated sediment/water or infected newts. Infectious elements are likely to be released onto
450 the skin surface and/or surrounding environment after mature cysts rupture as suggested by others
451 (Perez, 1913; Broz and Privora, 1952; Jay and Pohley, 1981). The transmission mechanisms of
452 *Dermocystidium spp.* between their fish hosts are well documented, where all species produce
453 zoospores to facilitate waterborne transmission (Perkins, 1976; Olson *et al.*, 1991). However, in this

454 study, both histological and TEM examinations consistently showed no sign of parasite spores
455 developing flagellae. In addition to direct skin exposure, the possibility of oral transmission cannot
456 be ruled out due to the microscopic observation of parasite cysts within the digestive system. This
457 might also explain the presence of liver cysts, which could pass through the bile duct following
458 ingestion as hypothesised previously (Raffel *et al.*, 2008). However, due to the anatomical location
459 of the liver, it is possible that parasite spores migrate through the sub-adjacent dermal-muscle layers
460 and into the liver.

461 Further studies are necessary to confirm the mode of parasite transmission and also to investigate
462 whether multiple infections, characterised by different developmental cyst stages within the same
463 individual, resulted from intra-tissue spread of mature infectious elements (*i.e.* merozoites type
464 elements released from mature cysts), or repeated external exposure where each cyst represents a
465 ‘discrete infection event’ as proposed by Raffel *et al.*, (2008).

466
467 To explore the variation in disease susceptibility several studies have considered the role played by
468 the innate immunity provided by antimicrobial peptides (AMPs) (Zaslof, 2002). Amphibian AMPs,
469 released from granular cutaneous glands are increasingly recognised as a first-line of defence
470 against pathogens that use the skin as their route of infection (Rollins-Smith *et al.*, 2002; Rollins-
471 Smith, 2009; Woodhams *et al.*, 2006; 2007). We speculate that the reduced diameter of granular
472 glands in infected newts, along with a partial depletion of these glands, could have a negative
473 impact on the production of AMPs, resulting in a partially compromised innate immune response
474 and increased susceptibility/severity to infection. Whilst we cannot allude to the mechanisms
475 leading to this difference, or the order of cause and effect, it is an interesting observation that may
476 deserve more investigation.

477 Based on the high sequence identity and phenotypic similarities, the pathogen observed here is the
478 same pathogen described from *L. helveticus* in Southern France (Gonzalez-Hernandez *et al.*, 2010).
479 Phylogenetic analysis not only emphasises their affiliation but also highlights their distinctiveness

480 from other species of Dermocystid. The well-supported and distinct clade containing the Rum and
481 France sequences, and the short branch lengths recovered under Bayesian analysis, are indicative of
482 a single species. Whilst the internal relationships between *Amphibiocystidium*, *Dermocystidium* and
483 *Rhinosporidium* species were not consistent across ML and Bayesian analysis, the amphibian and
484 fish infecting pathogens are not monophyletic. *Rhinosporidium sp.* formed a discrete clade
485 suggesting one evolutionary host-shift to mammalian hosts. However, the nested arrangement of
486 *Dermocystidium sp.* and *Amphibiocystidium spp.* suggests that pathogens can undergo host-shifts,
487 resulting in several, independent amphibian-specific lineages. Whilst host shifts between the lower
488 invertebrates are not uncommon (Densmore and Green, 2007; Bandín and Dopazo, 2011, Price *et*
489 *al.*, 2014), the presence of multiple host-shifts from fish to amphibians, but not the converse, is
490 atypical and appears to contradict previous theories on host-shifts (Jancovich *et al.*, 2010). In
491 agreement with Feldman *et al.* (2005) our analysis distinguished *A. penneri* from other
492 Mesomycetozoeans with high confidence, supporting its consideration as a separate genus.
493 Sequences from Rum and Larzac were also distinct from *Amphibiocystidium sp.*, instead forming a
494 clade with *A. penneri*, a pathogen of *B. americanus* in Northern America. The *L. helveticus*
495 infecting pathogens are therefore not members of *Amphibiocystidium*, but instead should be
496 consider a novel species within the genus *Amphibiothecum*; *Amphibiothecum meredithae*.

497

498 **ACKNOWLEDGEMENTS**

499 We gratefully acknowledge all the staff of the Easter Bush Pathology unit at the Royal (Dick)
500 School of Veterinary Studies for their technical assistance, in particular we are grateful to Ms
501 Jennifer Harris for performing microbiology tests. We are also grateful to Stephen Mitchell (Kings
502 Building) for assistance in TEM sample preparation and for support with TEM.

503

504 **FINANCIAL SUPPORT**

505 Work was supported by The Natural Environment Research Council (Grant number S055). Funding for
506 microbiology analysis came from The Royal (Dick) School of Veterinary Studies.

507 **REFERENCES**

- 508 Anderson, L. (2010) *Investigating the distribution and prevalence of a recently emerged parasite threatening*
509 *palmate newts (Lissotriton helveticus) on the Isle of Rum.* (Unpublished master's thesis) Institute of Zoology,
510 London.
- 511 Annis, S. L., Dastoor, F. P., Ziel, H., Daszak, P., Longcore, J. E. (2004) A DNA-based assay identifies
512 *Batrachochytrium dendrobatidis* in amphibians. *Journal of Wildlife Diseases*, **40(3)**, 420-428.
- 513 AVMA (2007) *American Veterinary Medical Association Guidelines on Euthanasia.* (Formerly the Report
514 of the AVMA Panel on Euthanasia) http://www.avma.org/issues/animal_welfare/euthanasia.pdf
- 515 Bandín, I. and Dopazo, C. (2011) Host range, host specificity and hypothesized host shift events among
516 viruses of lower vertebrates. *Veterinary Research* **42(1)**, 1-16
517
- 518 Berger, L. Speare, R. Daszak, P., Green, D. E., Cunningham, A. A., Goggin, C. L., Slocombe, R. Ragan, M.
519 A. Hyatt, A. D., McDonald, K. R. Hines, H. B., Lips, K. R., Marantelli, G. and Parkes, H. (1998)
520 Chytridiomycosis causes amphibian mortality associated with population declines in the rainforests of
521 Australia and Central America. *Proceedings of the National Academy of Sciences*, **95**, 9031-9036.
522
- 523 Berger, L., Speare, R. and Hyatt, A. (1999) Chytrid fungi and amphibian declines: overview, implications
524 and future directions. In *Declines and Disappearances of Australian Frogs* (ed. A. Campbell), pp. 21–31.
525 Environment Australia, Canberra, Australia.
526
- 527 Blaustein, A. R. and Wake, D. B. (1990) Declining amphibian populations - a global phenomenon. *Trends in*
528 *Ecology & Evolution* **5**, 203-204.
529
- 530 Blaustein, A.R., and Wake, D. B. (1995) The puzzle of declining amphibian populations. *Scientific American*.
531 **272**, 52-57.
532
- 533 Blaustein, A. R., Gervasi, S. S., Johnson, P. T. J., Hoverman, J. T., Belden, L. K., Bradley, P. W. and Xie, G.
534 Y. (2012) Ecophysiology meets conservation: understanding the role of disease in amphibian population
535 declines. *Philosophical Transactions of the Royal Society Biological Sciences*. **367(1596)**, 1688-1707.
536
- 537 Broz, O., and Privora, M. (1952) Two skin parasites of *Rana temporaria*: *Dermocystidium ranae* Guyenot et
538 Naville and *Dermosporidium granulorum* n. sp. *Parasitology* **42**, 65-69.
539
- 540 Clare, F., Daniel, O., Garner, T., and Fisher, M. (2016) Assessing the ability of swab data to determine the
541 true burden of infection for the amphibian pathogen *Batrachochytrium dendrobatidis*. *Ecohealth*, **13(2)**,
542 360-367
543
- 544 Courtois, E. A., Cornuau, J. H., Loyau, A., and Schmeller, D. S. (2013) Distribution of *Amphibiocystidium*
545 sp. in palmate newts (*Lissotriton helveticus*) in Ariège, France. *Herpetology Notes*, **6**, 539-543.
546
- 547 Daszak, P., Berger, L., Cunningham, A. A., Hyatt, A. D., Green, D. E., and Speare, R. (1999) Emerging
548 infectious diseases and amphibian population declines. *Emerging Infectious Diseases* **5**, 735-748.
549
- 550 Daszak, P., Cunningham, A. A., and Hyatt, A. D. (2000) Emerging infectious diseases of wildlife threats to
551 biodiversity and human health. *Science* **287**, 443-449.
552
- 553 Densmore, C. L., and Green, D. E. (2007) Disease of Amphibians. *Institute for Laboratory Animal Research*
554 *Journal* **48(3)**, 235-54.
555
- 556 Duffus, A. L. J. and Cunningham, A. A. (2010) Major Disease Threats To European Amphibians.
557 *Herpetological Journal*. **20(3)**, 117-127.
558

- 559 Feldman, S. H., Wimsatt, J. H., and Green D. E. (2005) Phylogenetic classification of the frog pathogen
560 *Amphibiothecum (Dermosporidium) penneri* based on small ribosomal subunit sequencing. *Journal of*
561 *Wildlife Disease*. **41**, 701-706.
- 562
563 Goodchild C. G., (1953) A subcutaneous, cyst-parasite of Bullfrogs: *Histocystidium ranae*, n. g. n. sp. *J.*
564 *Parasitol.***39**, 395-405.
- 565
566 Goodman, R. M., Miller, D. L., and Ararso, Y. T. (2013) Prevalence of Ranavirus in Virginia Turtles as
567 Detected by Tail-Clip Sampling versus Oral-Cloacal Swabbing. *Northeastern Naturalist*, **20(2)**, 325-332
568
- 569 González-Hernández, M., Denoël, M., Duffus, A.J.L., Garner, T.W.J., Cunningham, A.A., Acevedo-
570 Whitehouse, K. (2010) Dermocystid infection and associated skin lesions in free-living palmate newts
571 (*Lissotriton helveticus*) from Southern France. *Parasitology International* **59**, 344–350.
572
- 573 Greer, A. L., and Collins, J. P. (2007) Sensitivity of a diagnostic test for amphibian Ranavirus varies with
574 sampling protocol. *Journal of Wildlife Diseases*, **43(3)**, 525-532.
575
- 576 Gray, A. (2006) Infection of the palmate newt (*Triturus helveticus*) by a novel species of
577 *Amphibiocystidium* on the Isle of Rum, Scotland (Unpublished Master's Thesis). Institute of Zoology,
578 London.
579
- 580 Gray, M. J., Miller, D. L., and Hoverman, J. T. (2012) Reliability of non-lethal surveillance methods for
581 detecting Ranavirus infection. *Diseases of Aquatic Organisms*, **99(1)**, 1-6
582
- 583 Green, K., Converse, A., and Schrader, A. K., (2002) Epizootiology of sixty-four amphibian morbidity and
584 mortality events in the USA, 1996–2001. *Annals New York Academy of Sciences*, **969**, 329-339
585
- 586 Griffiths, R. A. (1996) *Newts and Salamanders of Europe*. London: T. & A.D. Poyser. 188 p.
587
- 588 Halliday T. R. (1990) The Evolution of Courtship Behavior in Newts and Salamanders. In: Peter, J. B.,
589 Slater J. S.R., and Colin B, editors. *Advances in the Study of Behavior* 19. San Diego: Academic Press, Inc.
590 pp 137–169.
591
- 592 Hall, T. A. (1999) BioEdit: a user-friendly biological sequence alignment editor and analysis program for
593 Windows 95/98/NT. *Nucliec Acids Symposium Series*, **41**, 95-98.
- 594
595 Han, B. A., Searle, C. L., Blaustein, A. R. (2011) Effects of an Infectious Fungus, *Batrachochytrium*
dendrobatidis, on Amphibian Predator-Prey Interactions. *PLoS ONE*, **6(2)**: e16675.
- 596
597 Hanlon, S. M., Lynch, K. J., Kerby, J., Parris, M. J. (201) *Batrachochytrium dendrobatidis* exposure effects
on foraging efficiencies and body size in anuran tadpoles. *Diseases of Aquatic Organisms*, **112**, 237–242
- 598
599 Herr, R. A., Ajello L., Taylor J.W., Arseculeratne S.N., and Mendoza L. (1999) Phylogenetic analysis of
600 *Rhinosporidium seeberi*'s 18S small-subunit ribosomal DNA groups this pathogen among members of the
protocystant myxomycetozoa clade. *Journal of Clinical Microbiology*, **3**, 2750–54
- 601
602 Hosmer, D. W., and Lemeshow, S. (2000) *Applied Logistic Regression*. New York, USA: John Wiley and
Sons.
- 603
604 Houlahan, J. E., Findlay, S. C., Schmidt, B. R., Meyer, A. H., and Kuzmin, S. L., (2000) Quantitative
Evidence For Global Amphibian Population Declines. *Nature*. **404**, 752-755.
- 605
606 Hyatt, A. D., Boyle, D. G., Olsen, V., Boyle, D. B., Berger L., Obendorf, D., Dalton A, Kriger, K., Hero, M.,
Hines H, Phillott R, Campbell, R., Marantelli, G., Gleason, F., and Colling, A. (2007) Diagnostic assays and

- 607 sampling protocols for the detection of *Batrachochytrium dendrobatidis*. *Diseases of Aquatic Organisms*, **73**,
608 175-192.
- 609 Jancovich, J. K., Bremont, M., Touchman, J. W., and Jacobs, B. L (2010) Evidence for Multiple Recent Host
610 Species Shifts among the Ranaviruses (Family *Iridoviridae*). *Journal of Virology*. **84(6)**, 2636-2647.
611
- 612 Larkin, M. A., Blackschiled, G., Brown, N. P., Chenna, R., McGettigan, P. A., McWilliam, H., Valentin, F.,
613 Wallace, I. M., Wilm, A., Lopez, R., Thompson, J. D., Gibson, T. J., and Higgins, D. G. (2007) Clustal W
614 and Clustal X version 2.0. *Bioinformatics*, **23(21)**, 2947-2948.
615
- 616 Lips, K. R. (1999) Mass mortality and population declines of anurans at an upland Site in Western Panama.
617 *Conservation Biology* **13**,117-25.
618
- 619 Lips, K. R., Brem, F., Brenes, R., Reeve, J. D., Alford, R. A., *et al.* (2006) Emerging infectious disease and
620 the loss of biodiversity in a Neotropical amphibian community. *Proceedings of the National Academy of
621 Sciences of the United States of America* **103(9)**, 3165–3170
- 622 Lindström K.M., van der Veen, I.T., Legault, B-A. and Lundström. J. O. (2003) Activity and predator escape
623 performance of Common Greenfinches *Carduelis chloris* infected with Sindbis virus. *Ardea* **91(1)**,103-111.
- 624 Longo, A. V., Burrowes, P. A., and Jogler, R. L. (2010) Seasonality of *Batrachochytrium dendrobatidis*
625 infection in direct-developing frogs suggests a mechanism for persistence. *Diseases of Aquatic Organisms*,
626 **92**, 253-60
- 627 Mendoza, L., Herr, R. A., Arseculerante, S. N., Ajello, L. (1999) In vitro studies on the mechanisms of
628 endospore release by *Rhinosporidium seeberi*. *Mycopathologia*, **148(1)**, 9-15
629
- 630 Mendoza, L., Taylor, J. W., and Ajello, L., (2002) The class Mesomycetozoea: a heterogeneous group of
631 microorganisms at the animal-fungal boundary. *Annual Reviews of Microbiology* **56**, 315–344.
632
- 633 Møller, A.P., Allander, K. and Dufva, R. (1990) Fitness effects of parasites on passerine birds: a
634 review. In: *Population Biology of passerine birds: An integrated approach*. (Blondel, J., Gosler, A.,
635 Lebreton, J.D. and McCleery, R.H. eds) pp 269-280. Berlin: Springer Verlag.
636
- 637 Olson, R.E., Dungan, C.F., and Holt, R.A. (1991) Water-borne transmission of *Dermocystidium salmonis* in
638 the laboratory. *Diseases of Aquatic Organisms* **12**, 41–48.
639
- 640 Pascolini, R., Daszak, P., Cunningham, A. A., Tei, S., Vagnetti, D., Bucci, S., Fagotti, A., and Di Rosa., I.
641 (2003) Parasitism by *Dermocystidium ranae* in a population of *Ranaesculenta* complex in Central Italy and
642 description of *Amphibiocystidium n. gen.* *Diseases of Aquatic Organisms* **56**, 65-74.
643
- 644 Pereira, C. N., Di Rosa, I., Fagotti, A., Simoncelli, F., Pascolini, R., and Mendoza, L. (2005) The pathogen
645 of frogs *Amphibiocystidium ranae* is a member of the order Dermocystida in the class Mesomycetozoea.
646 *Journal of Clinical Microbiology* **43**, 192-198.
647
- 648 Perez, C. (1907) *Dermocystidium pusula*, organismenouveau parasite de lapeaudestritons. *Comptesrendus de
649 seances de societe de biologie* **63**, 445-446.
650
- 651 Perez, C. (1913). *Dermocystidium pusula*: Parasite de la peau des Tritons. *Archives de Zoologie
652 Experimentale et Generale* **52**, 343–357.
653
- 654 Perkins, F. O. (1976) Zoospores of the oyster pathogen *Dermocystidiummarinum*. I. Fine structure of the
655 conoid and other sporozoan-like organelles. *Journal of Parasitology* **62**, 959-974.
656
- 657 Posada, D., and Crandall, K. A. (1998) ModelTest: testing the model of DNA substitution. *Bioinformatics*,
658 **14(9)**, 817-818.

- 659 Price, S. J., Garner, T. W. J., Nichols, R. A., Balloux, F., Ayres, C., Mora-Cabello de Alba, A. and Bosch, J.
660 (2014) Collapse of amphibian communities due to an introduced Ranavirus. *Current Biology* **24**, 2586-2591.
- 661 R Core Team (2015) R: A language and environment for statistical computing. R Foundation for Statistical
662 Computing. Vienna, Austria
- 663 Rambaut, A. (2014) Figtree, a graphical viewer of phylogenetic trees. Available from:
664 <http://tree.bio.ed.ac.uk/software/figtree>.
- 665 Raffel, T. R., Bommarito, T., Barry, D. S., Witiak, S. M., and Shackelton, L.A. (2008) Widespread infection
666 of the Eastern red-spotted newt (*Notophthalmus viridescens*) by a new species of *Amphibiocystidium*, a
667 genus of fungus-like Mesomycetozoon parasites not previously reported in North America. *Parasitology*
668 **135**, 203-215.
- 669 Ragan, M. A., Goggin, C. L., Cawthorn, R.J., Cerenius, I., Jamieson, A. V. C., Plourde, S. M., Rand, T. G.,
670 Soderhall, K., and Gutell, R. R. (1996). A novel clade of protistan parasites near the animal-fungal
671 divergence. *Proceedings of National Academy of Sciences USA*, **93**, 11907-11912.
- 672
673
674 Roelants, K., Gower, D. J., Wilkinson, M., Loader, S. P., Biju, S. D., Guillaume, K., Moriau, L., and Bossuyt,
675 F. (2007) Global Patterns of Diversification in the History of modern Amphibians. *Proceedings of the*
676 *National Academy of Sciences* **104(3)**, 887-892.
- 677
678 Rollins-Smith, L. A., Doersam, J. K., Longcore, J. E., Taylor, S. K., Shamblyn, J. C., Carey, C., and Zasloff,
679 M. A. (2002) Antimicrobial peptide defenses against pathogens associated with global amphibian declines.
680 *Developmental and Comparative Immunology*, **26(1)**, 63-72
- 681
682 Rollins-Smith, L. A. (2009) The role of amphibian antimicrobial peptides in protection of amphibians from
683 pathogens linked to global amphibian declines. *Biochimica et Biophysica Acta - Biomembranes*, **1788(8)**,
684 1593-1599.
- 685
686 Ronquist, F., and Huelsenbeck, J. P. (2003) MrBayes 3: Bayesian phylogenetic inference under mixed
687 models. *Bioinformatics*, **19(12)**, 1572-1574.
- 688
689 Rowley, J.J.L., Gleason, F.H., Andreou, D., Marshall, W., Lilje, O., and Goslan, R. (2013) Impacts of
690 Mesomycetozoon parasites on amphibian and freshwater fish populations. *Fungal Biology Reviews* **27**, 100-
691 111.
- 692
693 Schloegel, L.M., Daszak, P., Cunningham, A. A., Speare, R., Hill, B. (2010) Two amphibian diseases,
694 chytridiomycosis and ranaviral disease are now globally notifiable to World Organization for Animal Health
695 (OIE): an assessment. *Diseases of Aquatic Organisms*, **92**, 101-108.
- 696
697 Shin, J., Bataille, A., Kosch, T. A., and Waldman, B. (2014) Swabbing often fails to detect amphibian
698 Chytridiomycosis conditions of low infection load. *PLoS One*, **9(10)**: e111091
- 699
700 Smith, K.G., Lips, K. R., and Chase, J. M. (2009) Selecting for extinction: nonrandom disease-associated
701 extinction homogenizes amphibian biotas. *Ecology Letters*, **12**, 1069-1078.
- 702
703 Skerratt, L.F., Berger, L., Speare, R., Cashins, S., McDonald, K.R., Phillott, A., Hines, H., and Kenyon, N.
704 (2007) Spread of chytridiomycosis has caused the rapid global decline and extinction of frogs. *EcoHealth*
705 **4**, 125-134
- 706
707 St-Amour, V., and Lesbarreres, D. (2006) Genetic evidence of Ranavirus in toe clips: an alternative to lethal
708 sampling methods. *Conservation Genetics*, **8**, 1247-1250
- 709
710 Swofford, D. L. (2002) PAUP*. Phylogenetic Analysis Using Parsimony (*and Other Methods). Version 4.
711 Sinauer Associates, Sunderland, Massachusetts.

712

713 Svennblad, B., Erixon, P., Oxelman, B and Britton, T. (2006) Fundamental differences between the
714 methods of maximum likelihood and maximum posterior probability in phylogenetics. *Systematic Biology*.
715 **55**(1), 116-121

716 Thompson, J.D., (1997) The CLUSTAL_X windows interface: flexible strategies for multiple sequence
717 alignment aided by quality analysis tools. *Nucleic Acids Research*, **25**,4876-4882.

718

719 Vilela, R., and Mendoza, L. (2012). The taxonomy and phylogenetics of the human and animal pathogen
720 *Rhinosporidium seeberi*: A critical review. *Revista Iberoamericana de Micología*, **29** (4), 185–199
721

722 Whitaker, B. R., and Wright, K. Eds. (2001) *Amphibian Medicine and Captive Husbandry*. Krieger Pub. Co,
723 Florida p 89-110.
724

725 Woodhams, D.C., Rollins-Smith, L.A., Carey, C., Reinert, L. K., Tyler, M. J., Alford, R. A. (2006)
726 Population trends associated with skin peptide defenses against Chytridiomycosis in Australian frogs.
727 *Oecologia*, **146**(4), 531-540
728

729 Woodhams, D. C., Rollins-Smith, L. A., Alford, R. A., Simon, M. A. and Harris, R. N. (2007) Innate
730 immune defenses of amphibian skin: antimicrobial peptides and more. *Animal Conservation*, **10**(4), 425-428
731

732 Yang, Z., and Rannala, B. (2012) Molecular phylogenetics: principles and practice. *Nature Reviews*
733 *Genetics*, **13**, 303-314.
734

735 Zasloff, M. (2002) Antimicrobial peptides of multicellular organisms. *Nature*, **415**, 389 - 395

736

737

738

739

740

741

742

743

744

745

746

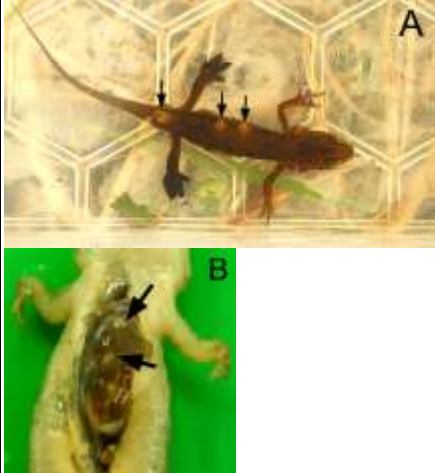
747

748

749

750 **TABLE LEGEND**

751 **Table 1. Description and gross lesions of *Amphibiothecum* sp. infection in *L. helveticus* on Rum**
 752

Type of lesions	Lesions description	Gross appearance
Type A	Spherical, 1- 3mm diameter, firm and raised clear to pale grey cystic lesions (arrows). Single or multiple, scattered or rarely clustered together. Present subcutaneously (A) and in the liver (B)	
Type B	Subcutaneous, firm, well-defined nodular swelling (from 1 up to 4 mm in diameter) associated with clusters of variable size (approx. <0.5mm to 1mm) white cysts (arrows).	
Type C	Subcutaneous irregular swelling up to 1 x 5 x 8 mm, with thinning of the skin and occasional cutaneous depigmentation, associated with cluster of pint-point (<1mm in diameter), slightly raised white lesions. Generally clustering (arrows)	
Type D	Subcutaneous clear fluid-filled vesicle/bullae (arrows) (up to 4 x 5 x 17 mm) with occasional <1mm diameter intralesional white cysts. Single but generally multiloculated. Often associated with severe widespread body oedema	

753
754

755

756

757 **FIGURE LEGENDS**

758 **Figure 1**

759 **Intradermal *Amphibiothecum sp.* cysts in palmate newt (*L. helveticus*).**

760 **A)** Cross-section of the trunk. Microscopic appearance of multiple spheroid cysts expanding and
761 distorting the *strata spongiosum* and *compactum* of the dermis. Cysts are surrounded by diffuse
762 and moderate subcutaneous oedema (*) associated with mild mixed inflammatory infiltrates. Scale
763 bar = 500 µm. Specific features: (C) cyst; (m) muscular fibers.

764 **Figure 2**

765 **A)** Longitudinal section of the tail. A large single developing *Amphibiothecum sp.* cyst expands the
766 *stratum spongiosum* of the dermis. The cyst lumen is filled with a myriad of basophilic immature
767 endospores. Note the absence of inflammatory cell infiltrate.

768 **B)** Cross-section of the trunk. The dermis and axial musculature are markedly expanded by the
769 presence of multiple coalescing cysts. Focal necrosis and moderate chronic inflammatory cell
770 infiltrate accumulates around (long arrow) or within (short arrow) the cysts. There is focal
771 epidermal hyperplasia (arrowhead).

772 **C)** Degenerating intradermal cyst surrounded by chronic active inflammation (arrows). The cyst
773 wall is distorted and partially detached from the host tissue by the presence of a clear space. Within
774 the cyst lumen, embedded in amorphous eosinophilic matrix, there are isolated islands of
775 polymorphic basophilic endospores and scattered endospores (arrowhead) which still retain the
776 morphological features observed in developing and mature cysts. Scale bar = 200 µm

777 **D)** Advanced stage of an intradermal degenerated cyst characterised by a granulomatous lesion.
778 Multinucleated giant cells (arrow), plasma cells and reactive fibroblasts surround a collapsed,
779 empty ellipsoid cyst.

780 **E)** Liver. Large hepatic granuloma consisting of a central empty cyst surrounded by concentric
781 layers of proliferating fibroblasts forming a fibrous wall. Admixed there are macrophages, scattered
782 lymphocytes and occasional multinucleated giant cells. There are subjectively increased number of
783 melanomacrophages (arrows) within the surrounding hepatic parenchyma.

784 **F)** Liver. Hepatic granulomatous lesion. The cyst lumen is partially replaced by moderate number
785 of foamy macrophages along with numerous multinucleated giant cells (arrows) and occasional
786 granulocytes. Few granular mature spores are observed within the cyst lumen or within local
787 macrophages. Inflammatory mixed cell infiltrate expands the surrounding oedematous hepatic
788 parenchyma.

789 Specific features: (C) Cyst; (ep) Epidermis; (g) Cutaneous granular gland; (ss) *Stratum spongiosum*
790 of the dermis; (w) Cyst wall; (m) Skeletal muscular fibers. Scale bar A, B, E= 500 μm ; C, D, F=200
791 μm

792 **Figure 3**

793 **A)** Cross-section of a developing intradermal *Amphibiothecum* sp. cyst containing myriad immature
794 endospores (IE). **B)** High power magnification of the inner lumen of a mature cyst. IE contained in
795 septate chambers (arrows) clustering at the inner periphery of the cyst wall.

796 **C)** Cross-section of intradermal *Amphibiothecum* sp. cyst containing both IE and ME. Clusters of
797 ME (long arrow) are opposite to IE (short arrow). Insert: ME and granular mature spores (circled).
798 Note few macrophages containing intracytoplasmic granular mature spores surrounding the outer
799 cyst wall (arrow). **D)** Subcutaneous dilated lymphatic vessel adjacent to a ruptured cyst. Granular
800 mature spores are free within the lumen (short arrows) or within macrophages (long arrows).
801 Specific features are indicated with lower case letters: (c) Cyst; (ep) Epidermis; (g) Cutaneous
802 granular gland; (ss) *Stratum spongiosum* of the dermis; (w) Cyst wall. Scale bar A, C= 200 μm ;
803 B=20 μm ; D= 50 μm

804 **Figure 4**

805 **Transmission electron microscope microphotograph of *Amphibiothecum* sp. intradermal cyst**
806 **from an infected palmate newt.**

807 Multiple endospores embedded in a thick electron dense fibrous and granular matrix (endospore
808 capsule) (M). Variable sized food vesicles (long arrows) and multiple dense round coarsely
809 osmiophilic granular inclusion bodies (short arrows) are occasionally present in cells protoplasm.
810 Membranous granular-fibrillar membranes (endospore membranes) forming concentric rings
811 around the protoplasm of each individual endospore (m). The right lower insert shows one
812 endospore dividing into four “daughter” cells. Encircled one visible nucleus with prominent
813 nucleolus.

814 **Figure 5**

815 **Consensus trees representing phylogenetic relationships of Mesomycetozoeans based on**
816 **18srRNA sequences.**

817 A) Maximum likelihood analysis implementing HKY+G+I with node support shown using
818 bootstrap support values; B) Bayesian inference run using reversible-jump MCMC to average over
819 the GTR models, with node support displayed as posterior probabilities; Amphibian-infecting
820 species are highlighted in red whilst sequences from Rum and Larzac are coloured blue.

821

822 **Supplementary materials:**

823 **Supplementary Figure 1A-D**

824 **Representative H&E stained section of extracutaneous locations of *Amphibiothecum* sp. cysts**

825 a) Parasite cyst within skeletal muscular fibres (arrow). b) Parasite cysts of the oral mucosa. Single
 826 intraluminal cyst (arrow) and several degenerating or degenerated sub-epithelial stromal cysts
 827 (arrowheads). c) Parasite cyst within the gastrointestinal lumen. d) Parasite cyst within the stroma
 828 of a male cloaca (arrow). Scale bar A, D=1000 µm; B=500 µm; C=200 µm

829

830 **Supplementary Table 1: Microbiological findings from 25 skin swabs obtained from control**
 831 **site (n=6) and from the infected sites (n=19).**

832

Type of culture	Intensity of colonies	Sample	<i>Pseudomonas fluorescens</i>	<i>P. luteola</i>	<i>Pseudomonas</i> sp.	<i>Burkholderia cepacia</i>	<i>Acinetobacter</i> sp.
MIXED	+	CTR (n=5)	1 (16.7%)	-	-	4 (66.7%)	-
	++		4 (66.7%)	-	-	-	-
	+++		-	-	-	1 (16.7%)	-
	+	INF (n=13)	-	5 (26.3%)	-	1 (5.3%)	1 (5.3%)
	++		10 (52.6%)	-	1 (5.3%)	5 (26.3%)	-
	+++		2 (10.5%)	1 (5.3%)	-	1 (5.3%)	-
PURE	+	CTR (n=1)	-	-	-	-	-
	++		-	-	-	-	-
	+++		-	-	-	1(5.3%)	-
	+	INF (n=6)	-	-	-	-	-
	++		4 (21%)	-	-	-	-
	+++		1 (5.3%)	-	-	1 (5.3%)	-

833

CTR=control site group; INF=infected sites group.

834

Observed intensity of colonies growth: +=few; ++=moderate; +++=heavy

835

Results are reported as percentage of observed growth

836

837 Skin swab samples from 6 newts in the control group and 19 from infected sites were used to

838 inoculate Horse blood agar (Oxoid PB0122A) and MacConkey agar (Oxoid PO0148A) plates.

839 Horse blood agar plates were incubated aerobically and anaerobically at 37 °C and Room

840 temperature and MacConkey agar plates were incubated aerobically as the same temperatures as

841 described above.

842 After 24 hours plates were examined and, if any predominant organisms was observed, these were

843 subbed onto fresh Horse Blood agar plates and incubated either at 37 °C or Room Temperature. The

844 following day the pure colonies were stained by Gram Stain and all were Gram negative bacilli.

845 These were subbed onto Nutrient agar plates for oxidase tests and used to inoculate API 20NE

846 (Biomérieux 20050) for identification.

847

848

849 **GenBank sequences used for sequence alignment and phylogenetic reconstruction**
850 *Dermocystida* sp. Larzac/B-m, GU232542.1; *Dermocystidia* sp. Larzac/C-f, GU232543.1;
851 *Rhinosporidium* sp. ex *Canis familiaris*, AY372365.1; *Rhinosporidium seeberi*, AF158369.1;
852 *Rhinosporidium cygnus*, AF399715.2; *Rhinosporidium seeberi*, AF118851.2; *Dermocystidium* sp.,
853 U21336.1; *Amphibiocystidium ranae* 2-04, AY692319.1; *Amphibiocystidium ranae*, AY550245.1;
854 *Amphibiocystidium* sp. C107, EU650666.1; *Dermocystidium* sp. CM-2002, AF533950.1;
855 *Dermocystidium salmonis*, U21337.1; *Amphibiocystidium* sp. *viridescens* LA1, EF493030.1;
856 *Amphibiocystidium* sp. *viridescens* MA1, EF493028.1; *Amphibiocystidium* sp. *viridescens* MA3,
857 EF493029.1; *Amphibiocystidium penneri*, AY772000.1; *Amphibiocystidium penneri*, AY772001.1;
858 *Dermocystidium percae* 35, AF533948.1; *Dermocystidium percae* 33, AF533946.1;
859 *Dermocystidium percae* 6, AF533944.1; *Dermocystidium percae* 1, AF533941.1; *Dermocystidium*
860 *percae* 5, AF533943.1; *Dermocystidium percae* 34, AF533947.1; *Dermocystidium percae* 9,
861 AF533945.1; *Dermocystidium percae* 4, AF533942.1; *Dermocystidium percae* 52, AF533949.1;
862 Uncultured eukaryote, AB275066.1.
863
864